Lund University

Department of Physics

Bachelor Thesis

May 7, 2018

Analysis of simulation of lightning in a cold-based convective storm

LUND UNIVERSITY
Faculty of Science

Author: Linus Karlsson

Supervisor: Vaughan Phillips

Co-supervisor: Elna Heimdal-Nilsson

Acknowledgement

I would like to dedicate my gratitude towards Vaughan Phillips who have been my supervisor during this project. Throughout these four months Phillips has offered me his knowledge and guidance and pushed me towards independence which has been a valuable experience for me as an apprentice scientist. During this project I have been encountering errors and problems of different kinds of nature which me and professor Phillips have discussed and worked through together.

Secondly, I would also like to thank Elna Heimdal-Nilsson who has been my co-supervisor and study advisor during my years at Lund University. Many thanks for all help you have offered me both throughout this project as well as during my time at Lund University.

Further I would like to thank Sachin Patade for his kindness to discuss and explain programming and computer related problems with me.

Lastly, I direct my appreciation and thankfulness to the department of Physical Geography at Lund University who have offered me a workstation with computer to work on during this project.

2018-05-07

Linus Karlsson

Table of content

Abbreviations

AC-Model	Aerosol-Cloud model
CAPE	Convective Available Potential Energy
MSL	Mean sea level
NetCDF	Network Common Data Form
STEPS	Severe thunderstorm electrification and precipitation study

A technical description of meteorological terms is given as the paper progress. A complementary glossary sheet is given in Appendix A which can be consulted while reading to support one that is not into the field.

Abstract

In this paper a simulation of a convective cell of a thunderstorm system observed 19th of June 2000 during the Severe Thunderstorm Electrification and Precipitation Study (STEPS) field campaign is being analysed. The storm system has been simulated with an Aerosol-Cloud model and the analysis is based on the output data. The analysis spans over 30 minutes which covers the mature stage and the beginning of the dissipation stage of the storm cell. A pronounced updraft is found in the centre of the cell with vertical wind speed reaching 17 m/s. The updraft ascends through a 'mixed-phased' region which is found at an altitude between 3 km to 9 km above mean sea level. The electrification of the storm cell is caused by microphysical species of ice attaining an electric charge due to rebounding collisions and rubbing against one another which gives rise to a charge separation. The analysis reveals that mainly ice particles and snow was found to be negatively charged while graupel positively. It was found that regions where the magnitude of the electric field is strongest is between regions of positive and negative charge which also coincides with the location where trigger points for light flashes were found. A total of 265 light flashes were found throughout a time period of 20 minutes which gives a rate of 13.25 light flashes per minute. A correlation between amount of lightning flashes and average magnitude of the electric field was found. It was found that the amount of lightning flashes increases as a result of the increased average magnitude of the electric field.

1. Introduction

Thunderstorms are powerful electrified cloud formations whose presence reveals the astonishing physical nature of the atmosphere. The vigorous forces that accompany thunderstorms have been estimated to cause more than 20 000 death and 200 000 injuries per year worldwide (Holle 2008). It has been estimated that damage caused on property and infrastructure due to lightning costs more than a billion dollars only in the United States yearly (NLSI). Thus, the importance of fostering thunderstorm research, atmospheric science and how the atmosphere operate cannot be neglected. The idea that different parts of a light emitting cloud attain either positively or negatively charged is widely known. Meanwhile many theories about how the actual electrification development of a cloud works are still being debated (Pruppacher *et al.* 1997).

Convective storm cells, if a favourable environment is present, can evolve into lightning producing thunderstorms (Stull 2000). These storm developments are complex systems. Forecasting thunderstorms requires advanced numerical models which ultimately resembles our current understanding of the atmospheric dynamics and physics. (Holton *et al.* 2013). Hence, as the hunt for new knowledge of the atmosphere continues, new pieces of information continue to contribute to a better understanding and allow our models to develop further. The puzzling scientific questions and search for answers of how thunderstorms develop and electrify are constantly in progress.

The vigorous forces that follows from a thunderstorm tend to have a capacity for disaster. Ranging from high wind speeds and intense rain showers to rock-solid hailstones and lethal lightning strikes, the consequences are many. To be naming a few, flooding, infrastructure- property- and agricultural-damage and even casualties frequently occur. Thus, the understanding of thunderstorms and how they function serves an important purpose to society and safety (Lang *et al.* 2004).

The present study is based on a model that simulates a storm system observed during the observational field campaign named *The Severe Thunderstorm Electrification and Precipitation Study (STEPS)*. It took place from May until July 2000 on the border line between Colorado and Kansas states in the United States (Lang *et al.* 2004). Specifically, a storm system that was observed and measured 19th of June 2000 is the subject of interest in which one storm cell is examined.

The purpose of this analysis is on first hand to examine what underlying elements that causes a convective updraft to evolve into a full-scale flash emitting thunderstorm. This is done by mapping where in the convective updraft cloud water, ice particles, snow and graupel are found and which electric charge each microphysical specie acquires. As a result, the present magnitude and location of electric fields aloft are of interest. To find out whether the convective updraft produces a flash it is examined if there is any charge density transferred to the cloud by the flash. The analysis is limited to only one convective updraft being analysed to understand in detail the sequence of microphysical events leading to lightning. Aerosols and chemistry that could affect the microphysical species has not been taken into consideration. As the analysis is based on model data, the model's validation is assumed to be reliable.

By finalizing this analysis, it is anticipated to contribute with material to the thunderstorm research community by which this analysis can be used as comparison material for further studies. Also, for future studies being conducted based on the STEPS observation this study can be used as background material.

The main resource to perform the analysis is by reviewing simulation output. Thus, evaluation of the data for this storm system makes up the basis of this project. The model used to run the simulation is an *Aerosol-Cloud (AC) model*. It is a model running in the three-dimensional room and utilizes a hybrid bin-bulk microphysical scheme. It essentially means that morphological properties for the different microphysical species are considered as well as the number and mass concentrations for each hydrometeor and aerosol in the cloud (Phillips *et al.* 2017). Further information about the AC-model is given in the Chapter 3, Section 3.1.

The following paper is designed such that a theoretical background is provided in Chapter 2 which consists of an overview of what is previously known. Next up in Chapter 3 is the methodology which includes an explanation of the AC-model used for the simulation and a description how the data was handled and the visualisation process of data. A short description of the case and environmental settings of the storm is given in this chapter too. Next is a result section which includes underlying creation process of each plot then a snapshot sequence follows with a description of shown events accompanied with discussion to the subject. The sequence of snapshots is followed up by showing time development of microphysical species and electrical properties. Finally, a chapter of conclusions that can be drawn from the study and an outlook of future work that can be done concludes the paper.

2. Background

2.1 Cloud physics and microphysical species

Microphysics is a collection of physical sciences about the microscopical scale (order of magnitude is typically micrometres). Cloud physics, a branch of microphysics, describes cloud development and the evolution of microphysical species. Microphysical species are branched into six main species which can be divided into two categories, *cloud-particles*, and *precipitation* (Rogers *et al.* 1989).

The cloud-particles are subdivided into:

- Water vapour (water in gas form).
- Cloud-droplet (water in liquid form with a size from 10 μm to 100 μm. Also referred to as cloud water in this paper.).
- Cloud-ice (frozen cloud-droplet, referred to as ice particle in this paper, also commonly called ice crystal)

The precipitation forms are defined as:

- Rain drop (water in liquid form with a size larger than 100 μm to approximately 5 mm).
- Snow (aggregate of cloud-ice)
- Graupel (Ice particle or snow that has grown due to collision with supercooled droplet, also referred to as accretion).

The transition between species and the growth due to thermodynamically processes are summarized in microphysical schemes. The basis of modern schemes is described in a paper by Lin (Lin *et al.* 1983). Thus, cloud physics provides a framework to understand and describe a thunderstorms development.

2.1.1 Convective dynamics

A convective updraft refers to an upward going wind. Thunderstorms consists of one or several updrafts, also called a storm cell, bringing humid air upwards. There are three main mechanics that causes air to move upwards. Orographic lifting, meaning that a physical object forces air upwards, for instance a mountain. Frontal lifting, meaning that two fronts of different temperatures, typically warm front and cold front collide. Thermal lifting, meaning that the surface of Earth is heated by the sun which lowers the density of the air causing it to move upwards as overlying colder air has higher density, also referred to an unstable air layer (Ahrens *et al.* 2015). A blob of air that is elevated is commonly referred to as an air parcel. The parcel concept is used in atmospheric science to describe movement of air. It entails properties such as it is a closed system meaning that no air is exchanged with the environment. As the parcel ascends, it expands due to decreased pressure which is followed by a decrease in temperature (Stull 2000). This relation is followed from the ideal gas law. When the parcel reaches saturation, meaning that further increase in water vapour content is not sustainable, water vapour starts to condense. The act of condensation releases latent heat which further heats the surrounding air allowing a parcel of air to elevate to great altitude. This forms the basis of an evolving cumulonimbus cloud which in turn can develop into a thunderstorm (Ahrens *et al.* 2015).

2.1.2 Microphysics

There are six main types of microphysical species as described in Section 2.1. There are two important aspects derived from microphysical species that applies to developing storm systems. First, the act condensation releases latent heat which fuels a developing storm due to the increased temperature which perturbates the stability of the atmosphere. Secondly, the growth and interaction of species explains precipitation and electrification accompanying a storm. Thus, the transition between them and how they affect one another is essential to understand development of storms (Lin *et al.* 1983).

Thunderstorms develop from cumulonimbus clouds. Due to the large vertical extent the temperature throughout is varying and the cloud top reach well below $0℃$. The region between $0℃$ and $-36℃$ is defined as a ‘mixed-phase region’ this refers to the fact that within this region water vapour, liquid water and solid ice can exist (Korolev *et al.* 2003). A schematic drawing of the mixed-phase region is shown in Fig. 1a. The liquid water exists in a so-called supercooled state. Upon impact with ice particles, snow, graupel in the cloud the supercooled droplets freeze, called heterogenous nucleation. Once a supercooled droplet enters a temperature below $-36℃$ there is no longer any need for a condensation nucleus for it to freeze, and it freeze spontaneously, called homogenous nucleation (Rogers *et al.* 1989). Supercooled droplets are found within the updraft region of a storm as ascending air is necessary to retain the liquid phase, preventing it from evaporating and transform into gaseous phase (Korolev *et al.* 2007).

The formation of precipitation differs depending in the temperature of the cloud base. A warm cloud base ($> 0℃$) produce precipitation through coalescence, where cloud droplets merge and form rain droplets. The opposite is called a cold cloud base ($< 0℃$) where the precipitation production is through the ‘ice crystal process’ (Rogers *et al.* 1989). This process describes the growth of ice particle due to vapour diffusion meaning that water vapour within close distance is supersaturated relative to the ice particle which is followed by condensation onto the ice particle which causes it to grow. A major difference between cold-based and warm-based clouds is that cloud droplets are too small to coalesce in cold-based clouds thus, growth of water in liquid phase is limited in cold-based clouds (Phillips *et al.* 2017). Another process that is abundant that otherwise is incorporated to understand the amount of ice particle fragments is

the Hallett-Mossop process (H-M process) (Mossop *et al.* 1974). This process is only active in warm-based clouds due to the requirement of cloud droplets that is larger than 24 μm which is not the case in cold-based clouds. Hence, the process that accounts for species growth in cold-based clouds is the ice crystal process.

2.2 Storm electrification

A widely accepted concept is that a cumulonimbus cloud evolves into a thunderstorm cloud as regions throughout the cloud acquire negative or positive charge. The charge layered structure is due to the microphysical species (ice particles, snow and graupel) getting charged through charge separation and due to the updraft wind speed, the species settle on different heights (Reynolds *et al.* 1957). The most common charge structure adopted is called a normal tripole where the mid-region of the cloud has a negative charge and positive charge above and below. A schematic drawing of a normal tripole can be seen in Fig. 1b. When the mid-region if found to be positively charged and negative above and below it is called an inversed tripole. This gives rise to an electric field due to the electric potential arising from the difference between negative and positive charge regions (Tessendorf *et al.* 2007).

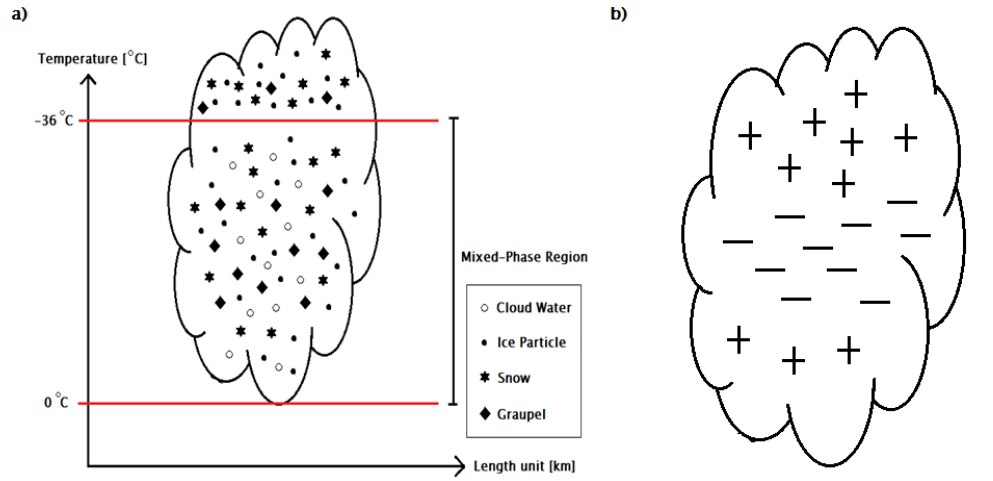

Fig. 1. *a) A schematic drawing of the mixed-phase region including which microphysical species that can be found within the region and at higher (colder) altitudes. b) A schematic drawing of a normal tripole electric charge structure in a cumulus cloud with a middle region charged negatively and an upper and lower region that is charged positively.*

Due to cloud obtaining a charge structure an electric field is present which is defined as,

$$\boldsymbol{E} = \frac{\boldsymbol{F}}{q} \tag{1}$$

Where $\boldsymbol{E} = (E_x, E_y, E_z)$ is the electric field, $\boldsymbol{F} = (F_x, F_y, F_z)$ is the coulomb force and q is the magnitude of the electric charge.

An electric field arise around an electrically charged object, such as an ice particle. Within the range of the electric field other charged objects are either attracted or repelled if charged oppositely or similarly respectively. Coulomb's law quantifies the strength of the attracting or repelling force within an electric field (Young *et al.* 2011).

Coulomb's law in scalar form is defined as,

$$F = k_e \cdot \frac{q_1 \cdot q_2}{r^2} \tag{2}$$

Where F is coulomb force (scalar), k_e is Coulomb's constant ($8.988 \cdot 10^9 \frac{N \cdot m^2}{C^2}$), q_1, q_2 are the magnitudes of the electric charges and r is the distance between the electric charges.

As a thunderstorm cloud acts in a three-dimensional space the magnitude of the electric field is acquired by,

$$E_{tot} = \sqrt{E_x^2 + E_y^2 + E_z^2} \quad (3)$$

Where E_{tot} is the magnitude of the electric field, E_x is the electric field in the x-direction, E_y is the electric field in the y-direction and E_z is the electric field in the z-direction.

To set the stage for thunderstorm development certain prerequisite must be met in terms of environmental conditions. A pronounced updraft (> 1 m/s) transports water vapour upwards and as the air get saturated it condenses into a cloud. A sufficient moisture content is necessary as it allows condensation to occur and thus, release of latent heat which acts as an engine of a convective cloud formation due to heating of air layer which leads to vertical movement. Also, an air layer that is unstable (warmer air laying underneath colder air) is necessary to start the development process (Stull 2000). A convective cloud (cloud with a vertical development) can extend to high altitudes where temperatures are well below zero degrees Celsius, until a temperature inversion (when the temperature increases with height) is met. The great depth of a convective cloud allows all forms of microphysical species to develop due to the wide range of temperature throughout and due to the capacity of the updraft to carry heavier species (Rogers *et al.* 1989).

Conventionally a convective cloud cells life cycle is divided into three stages, cumulus stage, mature stage, and dissipating stage. The cumulus stage is identified by an updraft throughout majority of the storm cell. As it advances into mature stage a well-defined downdraft also develops as well as precipitation. By the time the downdraft cuts off the lower part of the updraft and hence marks the start of the dissipating stage and the cumulus cloud dissolves from below (Rogers *et al.* 1989). A schematic sketch of a convective cloud cells life cycle can be seen in Fig. 2.

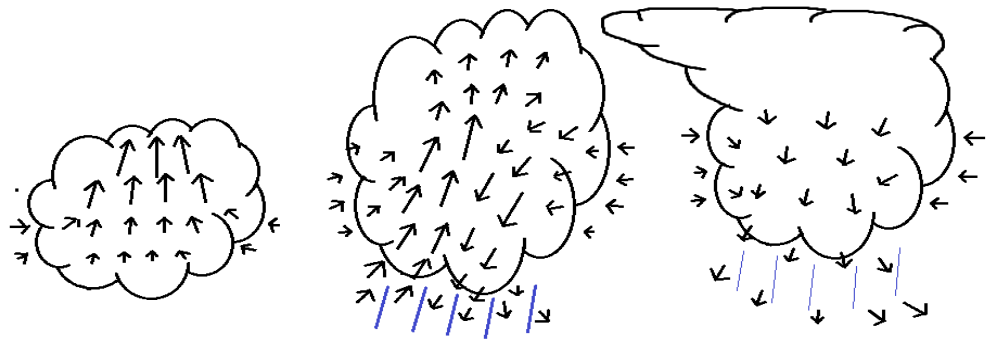

Fig. 2. *Schematic sketch of a convective cloud cells life cycle. From left: Cumulus stage with a pronounced updraft that transports humid air upwards. Mature stage where a downdraft has developed, and precipitation is at its peak. Dissipating stage where the updraft has ceased, precipitation has decreased, and the cloud is dissipating from below.*

2.2.1 Charge separation

Reynolds *et al.* (1957) suggested a charge separation mechanism which causes the crystal structured microphysical species, ice particles, snow and graupel to acquire electric charge due to rubbing and rebounding collision. It was suggested that graupel acquire charge through

collisions with ice particles as the graupel grow due to accretion, which is the growth from collision with supercooled droplets which freeze upon impact. Charge can also be obtained when two ice structures (ice particle, snow or graupel) rub against one another which was suggested that the warmer of the two attained a negative charge.

An extensive experimental study on charge separation was conducted by Takahashi *et al.* (1979) in which several environmental settings was constructed to identify whether riming processes (graupel) favoured positive or negative charge. The results from the experimental study suggested that both supercooled droplets and ice particles needs to be present in the environment (which was also found by Reynolds *et al.* (1957)) to enable any charge separation to occur during the event of colliding solid microphysical species. Further, the charge and magnitude were found to be dependent on temperature and cloud water content. The outcome of the study provided following boundaries: Independent on cloud water content, if temperature was higher than $-10℃$ graupel would acquire a positive charge. In environments with temperatures below $-10℃$ positive charged graupel was recorded in combination with low or very high cloud water content. However, cloud water content in between would result in a negatively charged graupel. The results are provided in graphical format in Fig. 3.

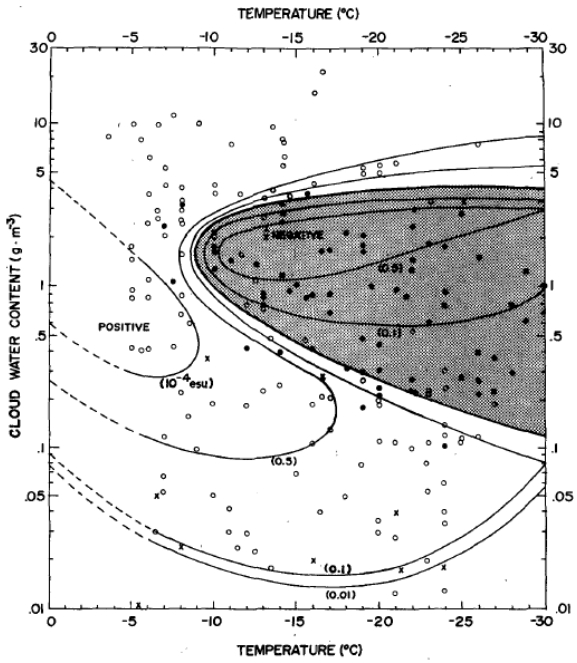

Fig. 3. *Results from Takahashi et al. (1979) paper where the open circles indicate graupel acquiring positive charge, solid circles indicate graupel acquiring negative charge and the crosses are cases where graupel was found uncharged. The white and grey regions indicate values which graupel is assumed to acquire positive and negative charge respectively.*

2.2.2 The lightning flash

For a lightning flash to form there needs to be oppositely charged regions, for instance a positive and negative region within a cloud (intra-cloud flash) or between cloud and surface (cloud to ground flash). Even between two clouds is possible (cloud to cloud flash). The electric charge difference creates an electric potential gradient between the regions meaning that an electric field develops. It is not completely understood which processes contribute to the formation of a lightning flash. One theory that has been used to describe its full life span is through dielectric breakdown of the air in the electric field. Once the electric field is large enough there is a

dielectric breakdown of the air, creating positive and negative ions and a lightning flash form. The build-up of the lightning flash occurs stepwise. First a positive and negative leader (ionized air) propagates away from the trigger point (location where a lightning discharge is initiated) parallel and antiparallel to the electric field vector. Second there is a branching of the leader and neutralisation of the charged regions. Once the positive/negative leader connects to region of negative/positive charge a lightning discharge forms and the previously charged regions are neutralised (Kitagawa *et al* 1960, Mansell *et al.* 2002).

3. Methodology

3.1 AC-model description

An AC-model was used to simulate the storm system. The simulation included the evolution of a wide variety of atmospheric variables, more of interest for this project was wind speed/direction, mass/number concentration of microphysical species and their electrical properties.

Spatial properties of the AC-model feature a cartesian coordinate system in which the grid space is designated a resolution of 1 km horizontally, 0.5 km vertically and 10 s temporal. The model output is however minutely based. Further, the storm line is aligned parallel to the *y*-axis and the propagation of the storm is parallel to the *x*-axis. The model domain is box-shaped and spans over 80 km west to east and south to north and vertically from mean sea level (MSL) to an altitude of 20 km. To account for the movement of the storm cell the model domain follows its movement, thus the model domain has a consistent speed of 9 m/s. The surface level of the region is at an altitude of 1.3 km which is accounted for by the model. (Phillips *et al.* 2017).

The AC-model was initialized with data (wind speed, wind direction, pressure, temperature, and humidity) from atmospheric sounding as well as aerosol profiles to perform the simulation. The sounding took place at the beginning of the simulation (2318 UTC 19 June 2000). The atmospheric sounding and aerosol profiles was used as input for the microphysical scheme. To account for evolution and interaction of microphysical species it utilizes a parameterization scheme (hybrid bin-bulk microphysics scheme) that treats collisions between solid microphysical species, essentially three types of collisions. 1: graupel colliding with graupel and/or graupel colliding with hail. 2: ice-particles and snow colliding with graupel/hail. 3. Collisions among ice-particles and snow. It also treats initiation of cloud water and ice particles. The AC-model was tested against the STEPS-observations to test the validity (Phillips *et al.* 2017).

Apart from mixing ratio and collision, charge density for the microphysical species is also treated including the electric field followed by the electric activity. Lastly the charge density transferred from a light flash to cloud is also included. Thus, the electric properties that the model handles provide a framework to analyse electric structure and lightning generation of the storm cell.

Validation of the model output in terms of microphysical species has been confirmed in studies by Phillips (2013, 2014, 2015 a,b and 2017). The electric properties that the model accounts for has been validated and will be published with an upcoming paper by Phillips. A more detailed description of the model is given in Phillips (2017) paper where it is applied in determining the role of ice multiplication.

3.2 Case and environmental conditions

The storm system that the AC-model simulates is a convective dry line (boundary between moist and dry air masses) that occurred 19th of June 2000 (early evening local time) on the border line between Colorado and Kansas states in the United States. It was measured and recorded during the Severe Thunderstorm Electrification and Precipitation Study (STEPS) (Lang *et al.* 2004)). The *STEPS-study* was a comprehensive study in which the objective was to study electrification and precipitation of storms. The location where the campaign was set was determined to be climatologically favourable for that kind of study. Measurements of the storm system were performed by a radar network (Doppler radar) to measure reflectivity of the storm system (spatial extension) as well as aircraft equipped with measurement probes to examine microphysical type and size. More about this study and its methodology can be read in a paper by Lang (2004).

Development had begun by 1000 UTC on the borderline between Colorado and Kansas. During the day surface temperatures of roughly 30℃ was reported and a dew point of $10℃ - 15℃$ on the east side of the dry line, indicating moister air compared to the western side that had a dew point of roughly 7℃. Due to the generally dry air the CAPE (Convective Available Potential Energy) was minimal. (CAPE is a measurement of how much energy that potentially can supply a convective updraft). The wind field was westerly to south-westerly leading to down shear on the eastern side of the storm system, (general propagation of the storm system was 71° clockwise from north (Phillips *et al.* 2017)). At 2300 UTC a new storm system emerged and was targeted by the STEPS operation centre. (Tessendorf *et al.* 2007). The AC-model simulates the period between 23:45 UTC to 02:15 UTC of this storm system.

The output data from the AC-model is stored in Network Common Data Form (NetCDF) format which is a collection of software libraries that creates data storing forms in which array-oriented scientific data can be stored and accessed by other software's. This format was especially developed for geosciences in which large amounts of data is collected and managed and thus, resulting in a common way to work with scientific data. More about NetCDF and its properties can be read at, www.unidata.ucar.edu/software/netcdf/.

The methodological approach for this study is provided in Fig. 4. The model output data (*x*, *y*, *z* and time values for each variable) is stored in one common data file (.nc format). The extraction of data for each variable was made through Fortran90 programs and then MATLAB scripts was used to visualize the data through plots. Code examples can be seen in Appendix B. The data was extracted in terms of horizontal and vertical slices to get an overview of the storm cells evolution. A conceptual visualization of the horizontal and vertical slice idea is shown in Fig. 5.

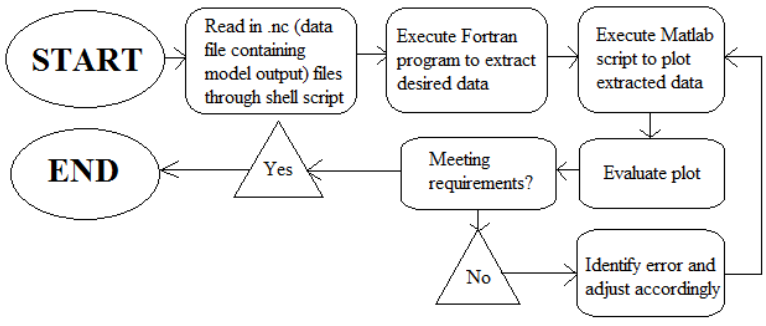

Fig 4. *Flowchart of the projects workflow. This work process has been performed for each individual plot.*

The workflow that is visualised in Fig. 4. was repeated for each individual variable that has been analysed. It consisted of three executable scripts. First a shell-script to extract a specific variable from a common data file. Then a Fortran90 script was used to extract a specific time-step of the variable that the shell-script extracted. Finally, a Matlab script was run to visualise the data extracted by the Fortran90 script. The visualisation (plot) that was produced was evaluated in terms of readability and providing the intended result desired to show. Thus, if these requirements were not met changes were made in the Matlab script where contour interval was adjusted.

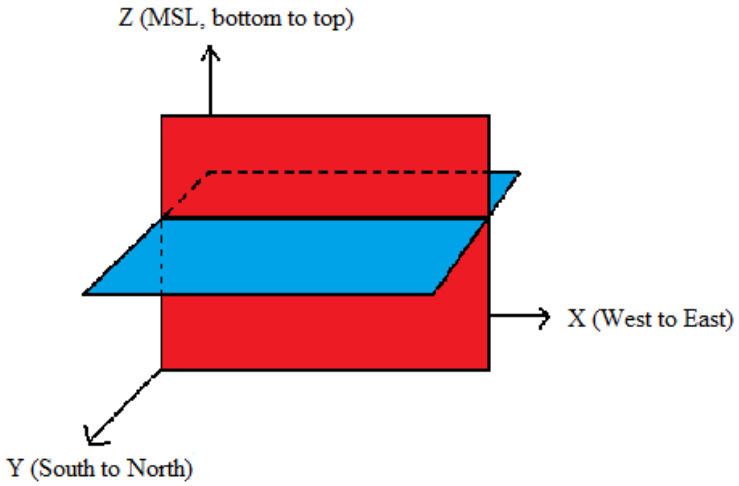

Fig. 5. *Conceptual visualisation of horizontal and vertical slice in the three-dimensional room. The blue plane and the red plane represent a horizontal slice and vertical slice respectively.*

4. Results

The result section is arranged such that first in Section 4.1, an explanation is given how each individual plot was constructed in terms of horizontal and vertical slices for each variable. In Section 4.2 the results are provided in the following order: Fig. 6 shows a horizontal overview of the storm cell in terms of vertical velocity. A cartoon of snapshots is provided in Fig. 7 through 14. Fig. 7, 9, 11 and 13 shows vertical slices of temperature, mass concentration mixing ratio of cloud water, snow and graupel, number concentration mixing ratio of ice particles and ice particle fragments. Fig. 8, 10, 12 and 14 shows charge density of ice particles, snow and graupel and their charge density combined, named total charge density, the magnitude of the electric field and the charge density transferred from flash to cloud. These figures are all relative to vertical velocity. Table 1 and 2 provides a summary of mass/number concentration mixing ratio peak values and average charge density peak values respectively. Fig. 15 and 16 shows time evolution of the average values of mixing ratios and electric variables. These values were conditionally averaged over the 'mixed-phase' region as this provides an overview of what is found in the region where charge separation is expected to occur. Lastly Fig. 17 shows the recorded trigger points for a 20-minute interval.

4.1 The process of visualising the results

Plots in Fig. 6 was constructed by extracting *x* and *y* values of vertical velocity for time-steps 85, 95, 105 and 115. Plots in Fig. 7, 9, 11 and 13 was constructed by extracting *x* and *z* values of vertical velocity/temperature and vertical velocity/microphysical specie for time-steps 85, 95, 105 and 115. Fig. 6 is a horizontal slice while Fig. 7, 9, 11 and 13 are vertical slices.

Charge density, magnitude of the electric field and charge density transferred to cloud from flash are presented in Fig. 8, 10, 12 and 14. Unlike Fig. 6, 7, 9, 11 and 13 these are averaged over ten vertical slices which gives an overview of the electric activity throughout the storm cell. Also, Pythagoras theorem was applied on the electric field to obtain magnitude instead of the electric field strength in each of the cartesian coordinates. Locations where trigger points were spotted are also provided in charge density transferred to cloud plots for time-steps 95 and 105.

Averaging the mixing ratio of the microphysical species was not considered relevant for this study as the highest concentration was assumed to be found in the region around the core of the updraft. The highest concentration was considered most relevant as it reveals the potential of how much charge can be generated through charge separation.

Fig. 15 and 16 are created by conditionally averaging values through time in the mixed-phase region where the updraft is found. This was defined as 30-50 km west to east direction and 3-9 km above MSL.

Fig. 17 was created from recorded trigger points by the model. The output received did however only contain data of trigger points up until time-step 105. Thus, only trigger points between time-steps 85 and 105 are shown. Also, the time resolution was 10 seconds thus, the flashes occurring between time-step 85 and 86 are all stored in time-step 85 and so on.

4.2 Analysis of results

Snapshot images of the evolution of the storm cell are provided from Fig. 6 to Fig 14 with an interval of ten minutes between each section. In total, a period of 30 minutes. This time-span was considered an appropriate time scale as it covers the entire mature stage, and the beginning of the dissipation stage for this storm cells life span. Further, the division into ten-minute section

was sufficient enough to cover the evolution of the microphysical species concentration as well as the charge density development and the electric activity.

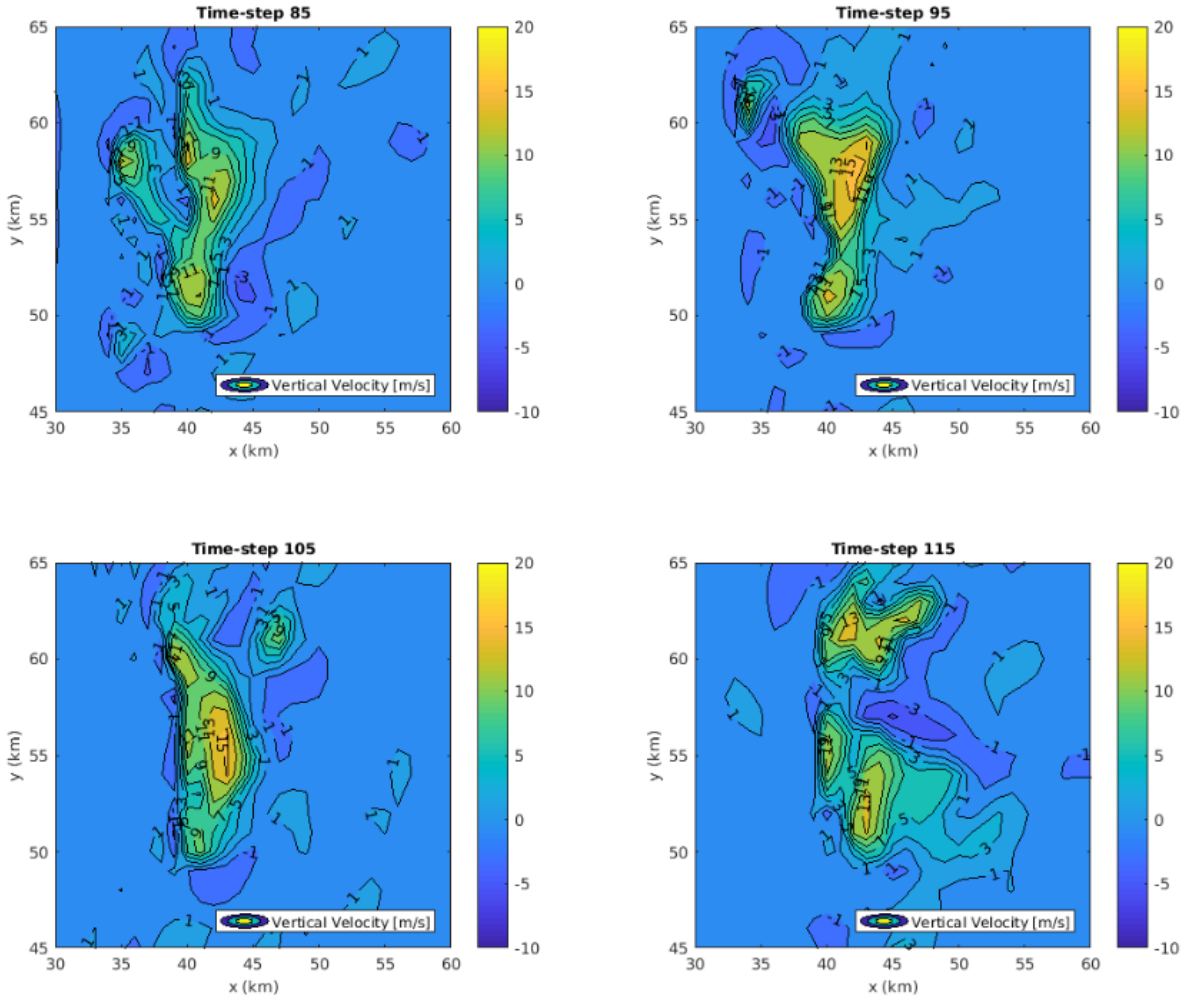

Fig. 6. *Horizontal sections of vertical velocity through the storm cell at the selected times of analysis. x-axis and y-axis represents west to east and south to north directions respectively. The altitude is set to 6.5 km above mean sea level. The time-steps shown are (from top left to bottom right) 85 (01:10 UTC), 95 (01:20 UTC), 105 (01:30 UTC) and 115 (01:40 UTC).*

The snapshots in Fig 6. shows the evolution of the storm cell in terms of vertical velocity at an altitude of 6.5 km above sea level. The air on this altitude has a temperature of roughly $-20°C$ which is suggested to be the centre of the ice crystal process (mixed-phase region) which is from 0 °C to $-36°C$. A critical boundary is the 1 m/s line which divides cumuliform clouds which has an updraft speed higher than 1 m/s from stratiform clouds that has an updraft speed lower than 1 m/s. It is important to distinguish between the two as a cumuliform clouds updraft speed has the capacity to accumulate and carry heavier hydrometeors hence this is where collision/charge separation is occurring. Starting from top left image, the cell is increasing in strength (time-steps 85, 95 and 105) until it is cut off by a downdraft to later dissipate (time-step 115).

The following plots found in Fig. 7, 9, 11 and 13 are vertical slices at the 56 km line, south to north direction (*y*-axis Fig 4). Plots found in Fig. 8, 10, 12 and 14 is an average of the values between 51 km and 61 km as seen in Fig. 6.

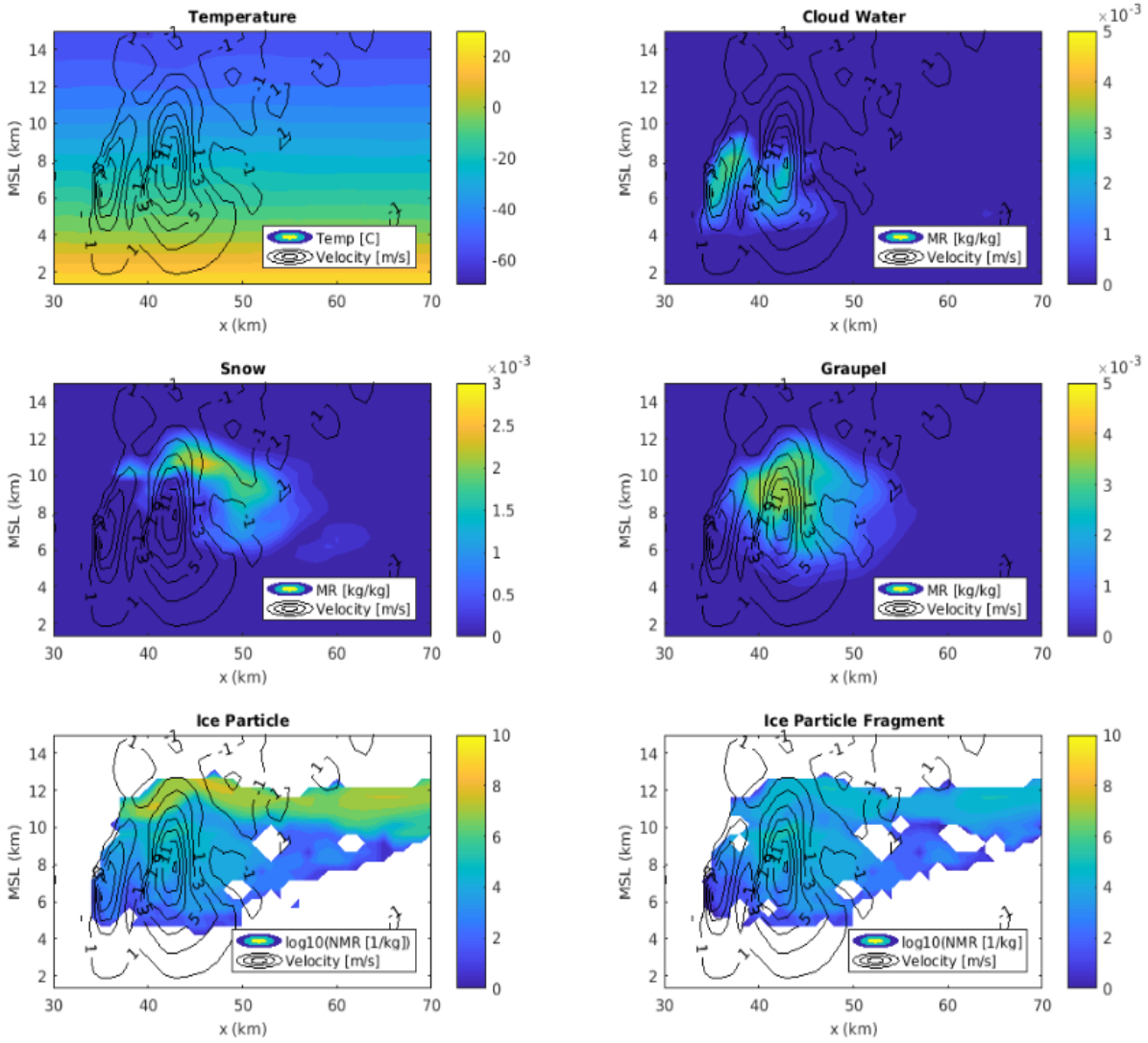

Fig. 7. *Time-step 85 (01:10 UTC): x-axis and y-axis represents west to east direction and altitude above mean sea level respectively. From top left to bottom right, temperature, mass concentration mixing ratio of cloud water, snow and graupel, logarithmic of number concentration mixing ratio of ice particles and ice particle fragments. All are relative to vertical velocity.*

The temperature field and mixing ratios of microphysical species for time-step 85 (01:10 UTC) are shown in Fig. 7. The updraft wind speed reaches up to 13 m/s and the mixed phased region is found at an altitude between 3 km and 9 km. Two regions of pronounced updraft winds can be seen. The cloud water is found within the updraft regions from 4 km to 9 km. This suggests that the cloud-base is found at a height of 4 km. Snow and graupel are found at altitudes between 5-6 km up until 12 km. Snow can be seen being accumulated at the top of the updraft and then carried away eastward by the westerly wind. Same can be seen for graupel including inside of the updraft. This is due to graupel being heavier than snow thus, graupel found within the updraft is heavier than what the wind speeds can carry. Ice particles and ice particle fragments are shown in logarithmic number concentration mixing ratio and can be found on altitudes between 5 km and 12 km. The region of high values of ice particles shows where cirrus clouds are found, which marks the top of the cumulonimbus cloud. Peak values of mixing ratios can be found in Table 1.

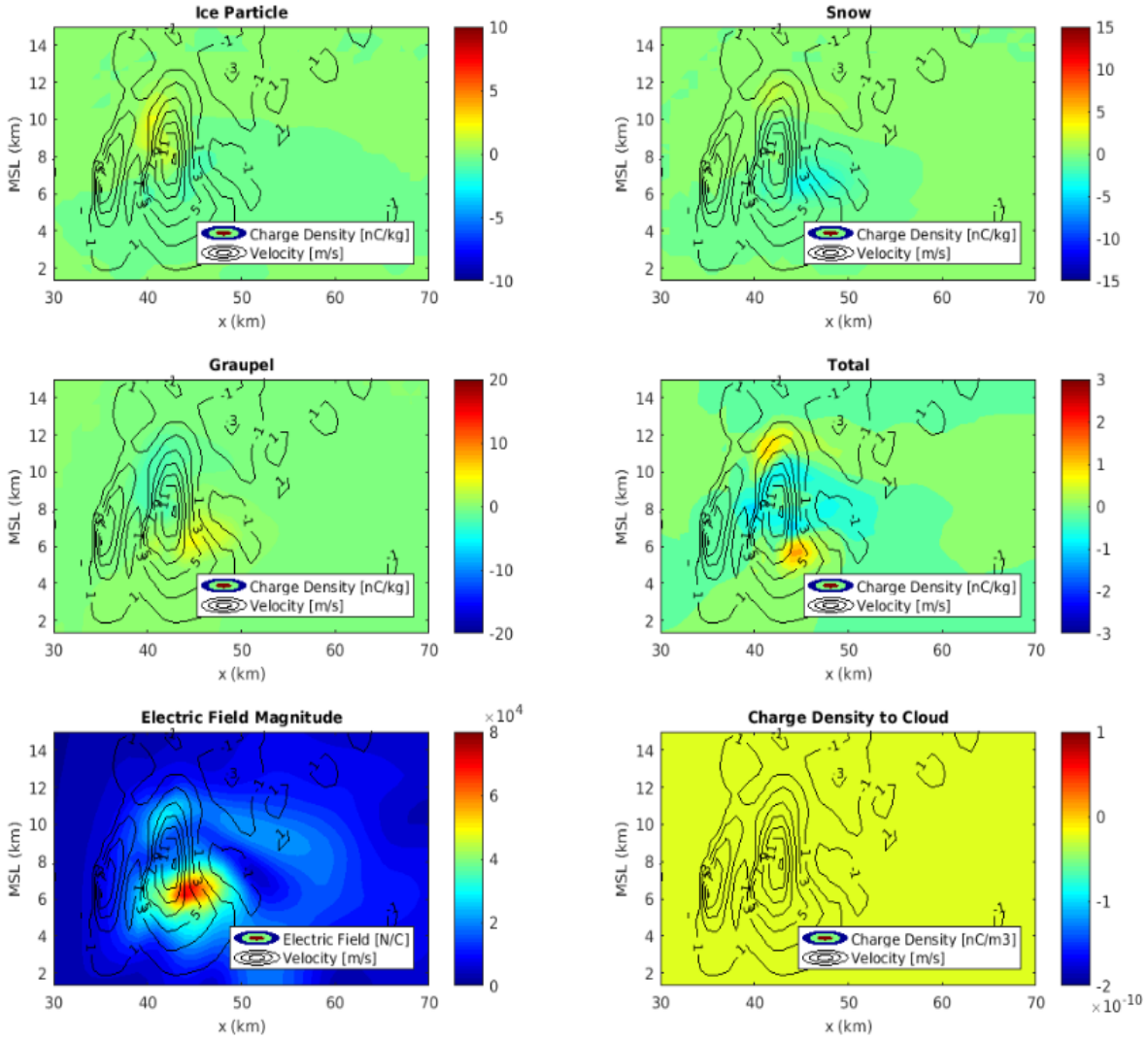

Fig. 8. *Time-step 85 (01:10 UTC). x-axis and y-axis represents west to east direction and altitude above mean sea level respectively. Charge density in ice particles, snow and graupel, as well as the total charge density resulting from these three microspecies combined are shown in the first four pictures. The magnitude of the electric field and charge density transferred from lightning flash to cloud is provided in fifth and sixth picture. All pictures are relative to vertical velocity.*

The electric variables for time-step 85 (01:10 UTC) are is shown in Fig. 8. The charge density of ice particles, snow and graupel are all found both positively and negatively charged. Graupel is found positively charged on altitudes between 5 km and 7 km on the east side of the updraft (downshear side) and negatively between 7 km and 12 km inside of the updraft. Ice particles and snow are found to be oppositely charged compared to which charge graupel has acquired. The total charge density shows a negative region in the middle between two positive regions which is referred to a normal tripole structure. The electric field appears to be strongest between lower positively charged region and the negatively charged region. No lightning flashes was recorded due to zero charge density transferred from flash to cloud.

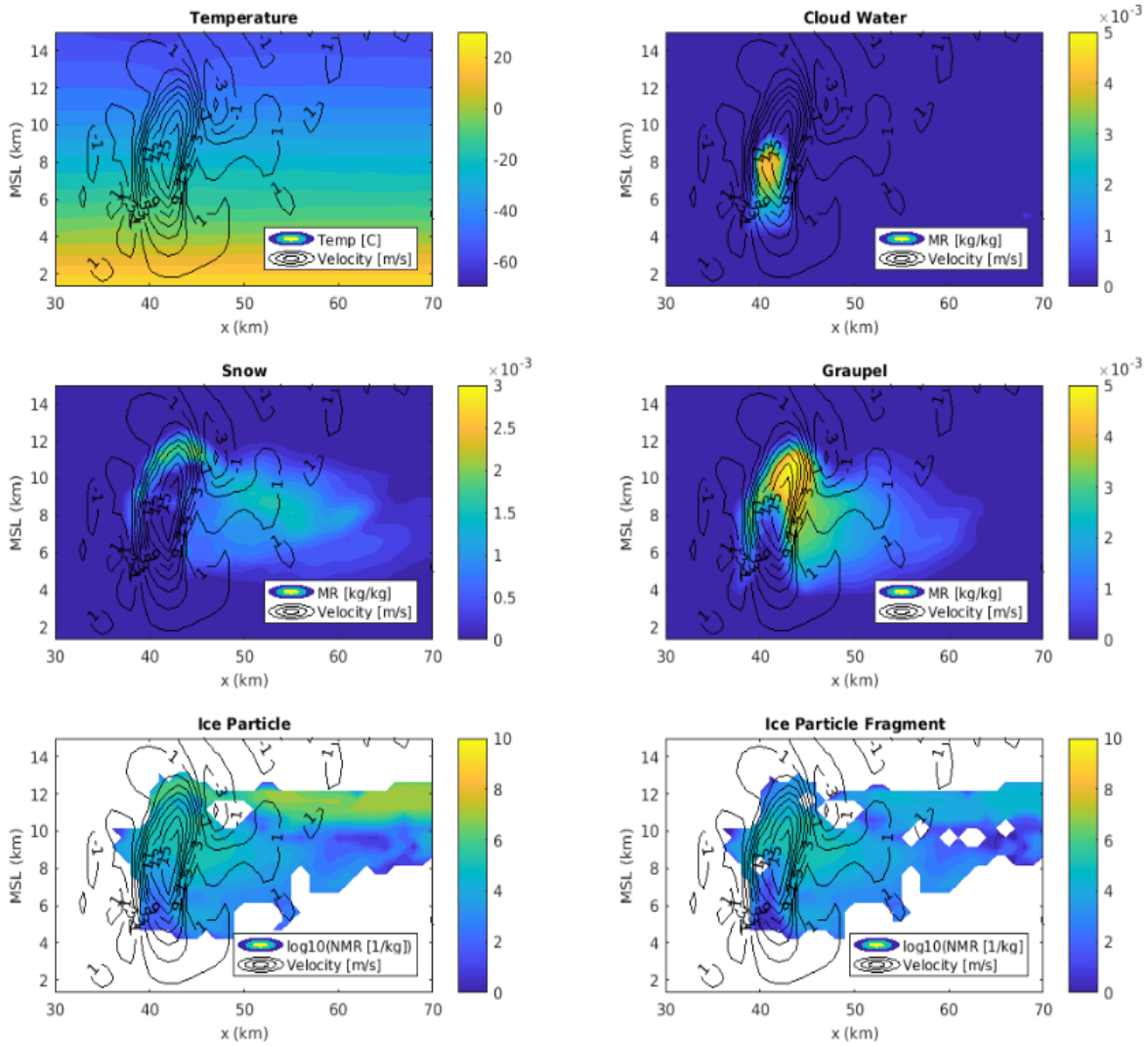

Fig. 9. *Time-step 95 (01:20 UTC): x-axis and y-axis represents west to east direction and altitude above mean sea level respectively. From top left to bottom right, temperature, mass mixing ratio of cloud water, snow and graupel, logarithmic of number mixing ratio of ice particles and ice particle fragments. All are relative to vertical velocity.*

The temperature field and mixing ratios of microphysical species for time-step 95 (01:20 UTC) are shown in Fig. 9. Updraft wind speed is now reaching 15 m/s and the previously two updraft regions has reduced to one. The mixed phase region is found on an altitude between 3 km to 9 km. The mass concentration mixing ratio of cloud water and graupel has increased since time-step 85 while snow has decreased. Both graupel and snow are now found on altitudes between 4 km up until 12 km and are also carried further eastward than previously. The number concentration of ice particles and ice particle fragments remain spread out over the region but a decrease in ice particles higher than 10 km altitude can be seen. Peak values of mixing ratios can be found in Table 1.

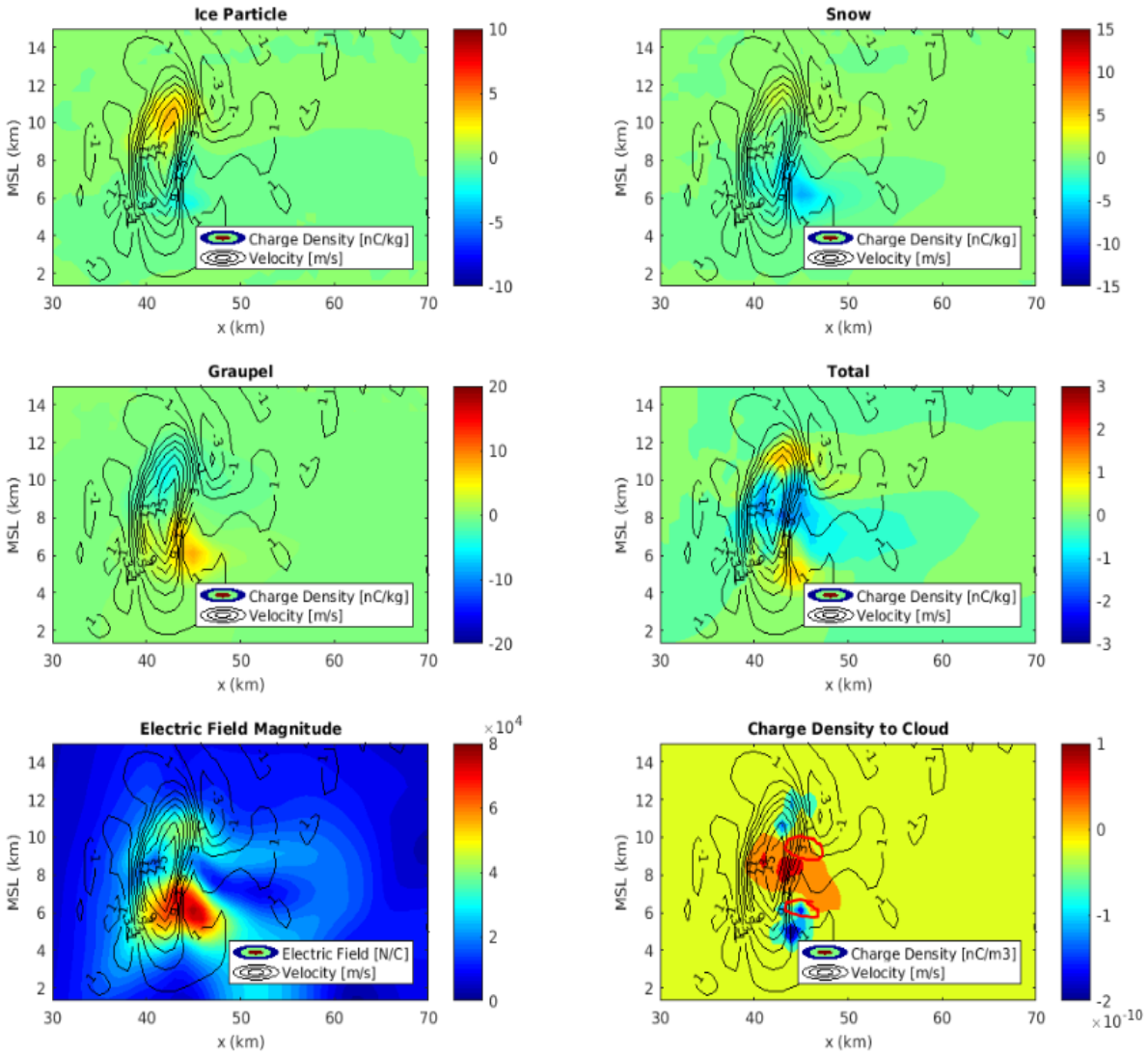

Fig. 10. *Time-step 95 (01:20 UTC). x-axis and y-axis represents west to east direction and altitude above mean sea level respectively. Charge density in ice particles, snow and graupel, as well as the total charge density resulting from these three microspecies combined are shown in the first four pictures. The magnitude of the electric field and charge density transferred from lightning flash to cloud is provided in fifth and sixth picture. The red circles in charge density to cloud picture is where trigger points were found. All pictures are relative to vertical velocity.*

The electric variables for time-step 95 (01:20 UTC) are shown in Fig. 10. Charge density for ice particles, snow and graupel has increased and still consists of a mixture of positive and negative charges. The electric charge structure remains similar as time-step 85. The electric field is more pronounced than previously and is found in the same region. Charge density transferred to cloud indicates that flash lightning activity was recorded, and the red circles indicate where trigger points were found. The magnitude of the electric field is found to be highest at locations where trigger points were found.

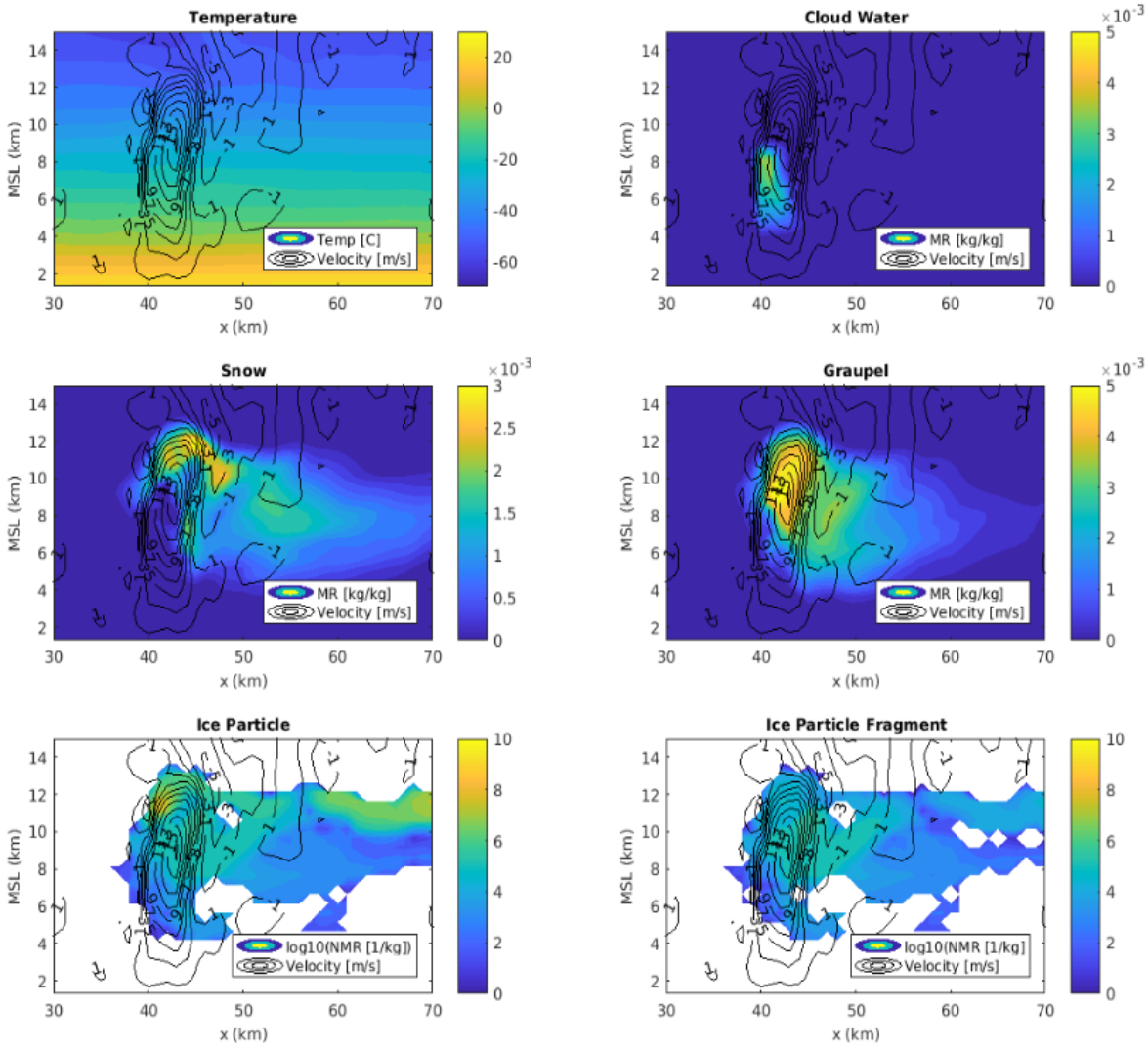

Fig. 11. *Time-step 105 (01:30 UTC): x-axis and y-axis represents west to east direction and altitude above mean sea level respectively. From top left to bottom right, temperature, mass mixing ratio of cloud water, snow and graupel, logarithmic of number mixing ratio of ice particles and ice particle fragments. All are relative to vertical velocity.*

The temperature field and mixing ratios of microphysical species for time-step 105 (01:30 UTC) are shown in Fig. 11. Updraft wind speed is now reaching 17 m/s. The mixed phase region is found at an altitude between 3 km to 9 km. The mass concentration of cloud water mixing ratio has decreased which means that the supply of supercooled droplet necessary for charge separation is weakened. Snow and graupel covers larger regions now and measure high concentrations of mass mixing ration. Ice particles and ice particles fragments remain throughout large regions. Peak values of mixing ratios can be found in Table 1.

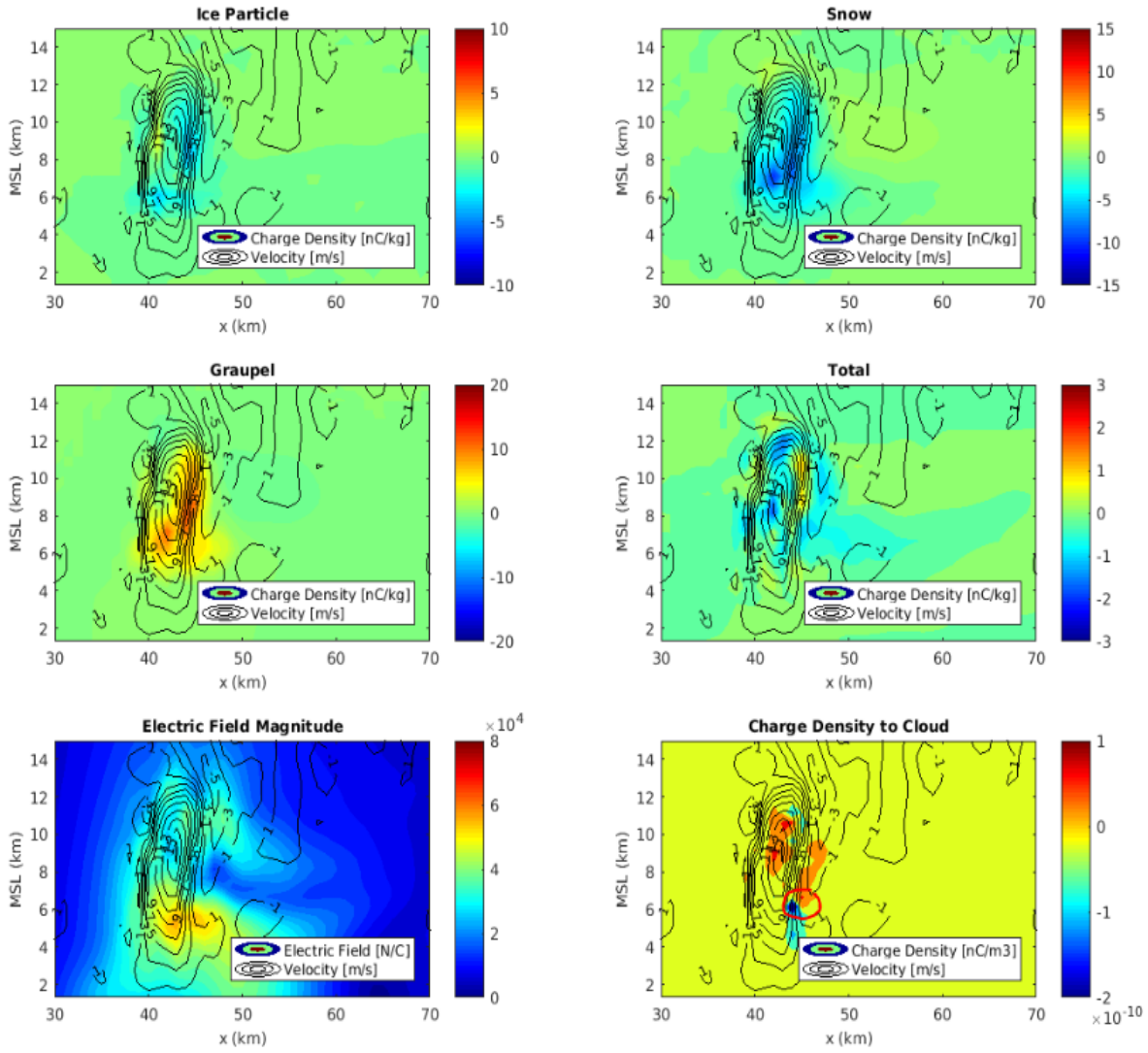

Fig. 12. *Time-step 105 (01:30 UTC). x-axis and y-axis represents west to east direction and altitude above mean sea level respectively. Charge density in Ice particles, Snow and Graupel, as well as the total charge density resulting from these three microspecies combined are shown in the first four pictures. The magnitude of the Electric Field and charge density transferred from lightning flash to cloud is provided in fifth and sixth picture. The red circle in charge density to cloud indicate where trigger points were found. All pictures are relative to vertical velocity.*

The electric variables for time-step 105 (01:30 UTC) can be seen in Fig. 12. At this time-step it is shown how ice particles and snow has attained almost entirely negative charge density while graupel positive charge. The electric charge structure deviates from previous time-steps and has a positively charged crack can be seen breaking through an otherwise completely negatively charged region. The electric field is weakened compared to previous time-steps and the charge density transferred to cloud suggests that flash lights are emitted. The trigger points found are indicated by the red circle in the charge density to cloud plot.

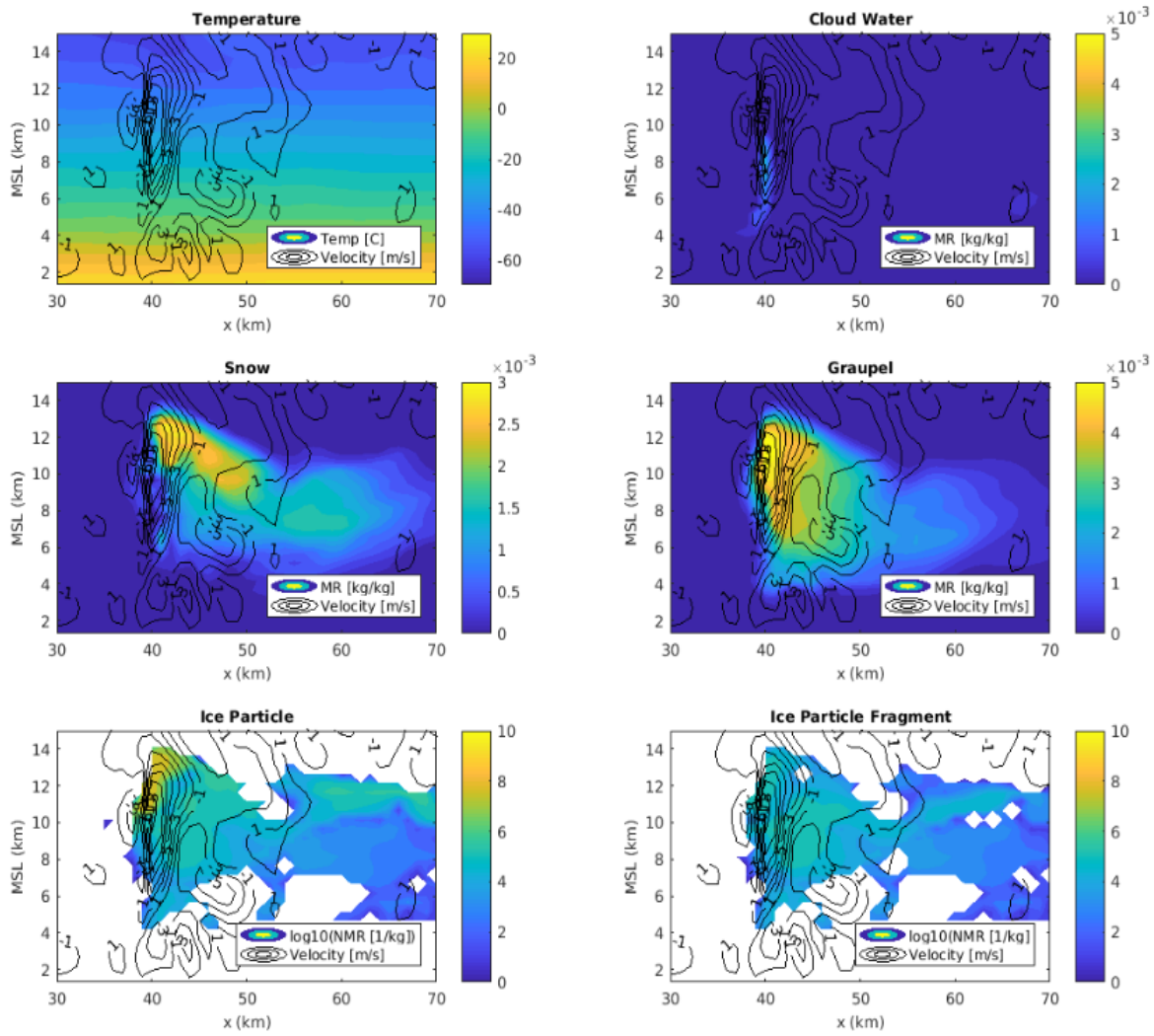

Fig. 13. *Time-step 115 (01:40 UTC): x-axis and y-axis represents west to east direction and altitude above mean sea level respectively. From top left to bottom right, temperature, mass mixing ratio of cloud water, snow and graupel, logarithmic of number mixing ratio of ice particles and ice particle fragments. All are relative to vertical velocity.*

The temperature field and mixing ratios of microphysical species for time-step 115 (01:40 UTC) are shown in Fig. 13. The mixed phase region is still found on an altitude between 3 km and 9 km. The updraft wind speed has subsided and reaches a magnitude of 13 m/s. Further a pronounced downdraft can be seen cutting through the lower region of the previous updraft core meaning that the dissipating stage of the cloud has begun. Cloud water has almost ceased to exist in the updraft core while ice particles, ice particles fragments, snow and graupel covers large regions including large regions of the downshear side. Peak values of mixing ratio values can be found in Table 1.

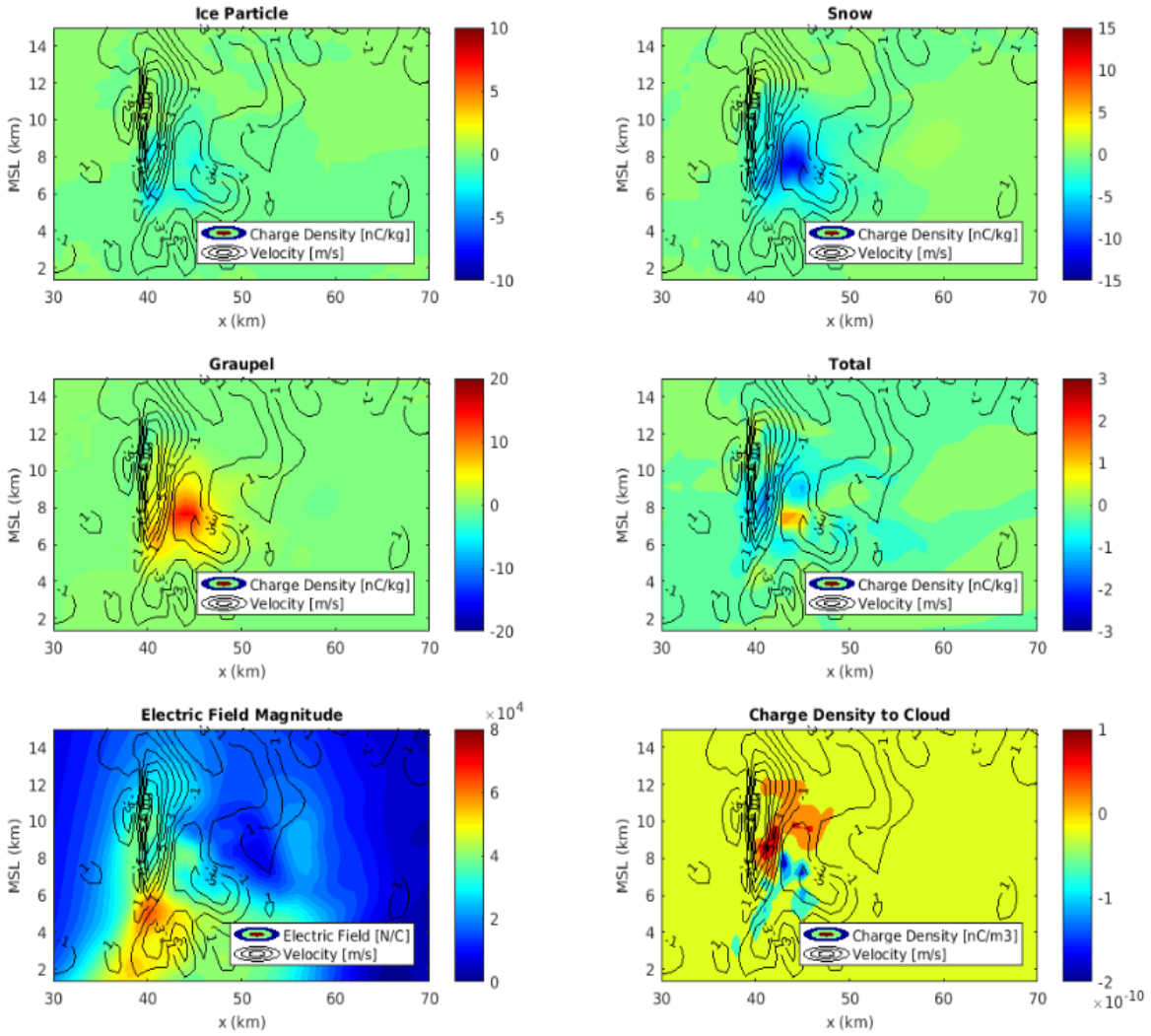

Fig. 14. *Time-step 115 (01:40 UTC). x-axis and y-axis represents west to east direction and altitude above mean sea level respectively. Charge density in ice particles, snow and graupel, as well as the total charge density resulting from these three microspecies combined are shown in the first four pictures. The magnitude of the Electric Field and charge density transferred from lightning flash to cloud is provided in fifth and sixth picture. All pictures are relative to vertical velocity.*

The electric variables for time-step 115 (01:40 UTC) can be seen in Fig. 14. Ice particles and snow are entirely negatively charged and graupel positively. The charge densities of graupel and snow are pronounced and has attained higher values than previously. This seems to be correlated to the high mass mixing ratio which can be seen in Fig. 13. The electric structure as now has one region of positive charge and is encapsulated by negative charge. The charge density to cloud suggests that light flashes is emitted during this time-step.

Table 1. *Summary from Fig. 7, 9, 11 and 13 of peak values of mass concentration mixing ratio (g/kg) for cloud water, snow and graupel as well as the logarithmic value of number concentration mixing ratio log10(1/kg) in the mixed-phase region for ice particles and ice particle fragments and they added.*

Specie (time-step)	$*_1$ (g/kg)	Specie (time-step)	$*_2$ log10(1/kg)
Cloud water (85)	3	Ice particle (85)	5
Cloud water (95)	4	Ice particle (95)	6
Cloud water (105)	3.5	Ice particle (105)	6
Cloud water (115)	2	Ice particle (115)	6
Snow (85)	2.5	Ice particle fragments (85)	5
Snow (95)	2	Ice particle fragments (95)	6
Snow (105)	2.5	Ice particle fragments (105)	6
Snow (115)	2.5	Ice particle fragments (115)	6
Graupel (85)	3.5	Ice particle + fragments (85)	10
Graupel (95)	4	Ice particle + fragments (95)	12
Graupel (105)	4.5	Ice particle + fragments (105)	12
Graupel (115)	5	Ice particle + fragments (115)	12

($*_1$: Peak mass concentration mixing ratio. $*_2$: Peak logarithmic number concentration mixing ratio in mixed-phase region)

The peak values of mixing ratios of the microspecies can be seen in Table 1. Cloud water reaches its peak at time-step 95, snow is more consistent through time with its lowest value at time-step 95 and graupel is steadily increasing reaching the peak at time-step 115. Ice particles and ice particle fragments through time has an almost consistent peak value. The decreased amount of cloud water suggests that it freeze to form ice particles as well as riming onto snow and ice particles to form graupel. The decline is also likely to be due to the downdraft cutting through the lower part of the updraft (as seen in time-step 115) thus, supply of new cloud water is weakened.

The cloud water content as seen in Fig. 9 reveals that the cloud base is found at roughly 3-4 km height. Comparing to the temperature field this is where the temperature turns negative indicating that it is a cold-based cloud. Hence, the ice-crystal process is suggested to be the dominant process for microphysical species to grow.

Fig. 8, 10, 12 and 14 shows the charge density in ice particles, snow and graupel as well as the total which accounts for the contribution from each. Also, the magnitude of the electric field and charge density transferred to cloud from lightning flash is shown in these figures. Table 2 provides an overview of the evolution through time of charge density sign and peak magnitude each microphysical specie attain.

Table 2. *Overview of peak charge density evolution (Fig 8, 10, 12 and 14) for ice particles, snow and graupel.*

Charge sign /Specie (time-step)	Positive, Peak charge density (nC/kg)	Negative, Peak charge density (nC/kg)
Ice Particle (85)	2	1
Ice Particle (95)	4	2
Ice Particle (105)	Very small	4
Ice Particle (115)	Null	3
Snow (85)	1	4
Snow (95)	1	7
Snow (105)	Very small	10
Snow (115)	Null	13
Graupel (85)	5	3
Graupel (95)	7	4
Graupel (105)	10	Null
Graupel (115)	15	Null

As seen in Table 2, a dual-sign charge density was observed for all microspecies during the first two time-steps, 85 and 95. At Time-step 105 and 115 ice particles and snow were found having a negative charge (time-step 105 has a very small and weak region of positive charge that is considered neglectable) while graupel positive. Comparing ice particles to snow the ice particles have a higher positive charge density than negative while the vice versa is true for snow, yet they both adapt a negative charge density for the last two time-steps.

In Fig. 8, 10, 12 and 14 a correlation between microphysical specie and charge compared to one another can be seen. It was found that regions where graupel is positively/negatively charged, ice particles and snow was found to be negatively/positively charged. This suggests that graupel is dominating within positively charged regions of the cloud while snow and ice particles is dominating within the negatively charged parts.

As suggested by Takahashi (1979), both cloud water and ice particle presence are necessary for charge separation to occur. As cloud water decrease the potential charge separation event also diminish. Further Takahashi (1979) suggested that graupel is always charged positively when found at temperatures higher than $-10℃$. This temperature is found at an altitude of 7 km as seen in Fig. 7, 9, 11 and 13. Looking at which charge density graupel has acquired it can be seen in time-step 85 and 95 that graupel is charged positively at altitudes below 7 km and charged negatively above while time-steps 105 and 115 shows that all graupel is charged positively. Thus, it is consistent with what Takahashi (1979) suggested that graupel found at temperatures higher than $-10℃$ is always positively charged. Looking at the region in time-step 85 and 95 where graupel was found to be negatively charged we can see that the average mass concentration mixing ratio of cloud droplets (Fig. 15) in those regions is between 0.7 g/kg and 0.5 g/kg and the temperature is between $-10℃$ to $-30℃$. The standard average density at this altitude is roughly 0.6 kg/m^3 (Holton 2013). Thus, multiply 0.6 kg/m^3 with 0.7 g/kg and 0.5 g/kg yields 0.42 g/m^3 and 0.3 g/m^3 respectively. Comparing these values to Fig. 3 we can see that it coincides with where Takahashi (1979) also recorded negative values. However further decrease in average mass concentration mixing ratio of cloud water would result in positively charged graupel at the lower temperatures which explains why we find positively charged graupel at time-step 105 and 115.

The electric structure (total charge density) varies throughout time. Time-steps 85 and 95 shows a structure where the middle section consists of negative charge and above and below positive charge. At time step 105 a trail of positive charge can be seen cracking through an overall negatively charged region. The last time-step, 115 the previously three-layer electric structure has reduced to a positive region that has an encapsulated structure of negative charge around it. Thus, time-step 85 and 95 has a standard tripole structure which its transforming into a more complex tripole structure where the last time-step almost resemble an inversed tripole structure.

The regions where the magnitude of the electric field is strongest are found in regions between positive and negative charge density of both total charge density and charge density transferred to cloud. The magnitude of the electric field from the electric activity seems to cease and spread throughout as the storm evolve. Further there seems to be an increased level of electric field between surface and cloud at a later stage of the storm. This suggests that the electric potential increase between cloud and surface at time-step 105 and 115 meaning that a discharge could occur between surface and cloud compared to previous time-steps where an intra-cloud discharge would be more likely.

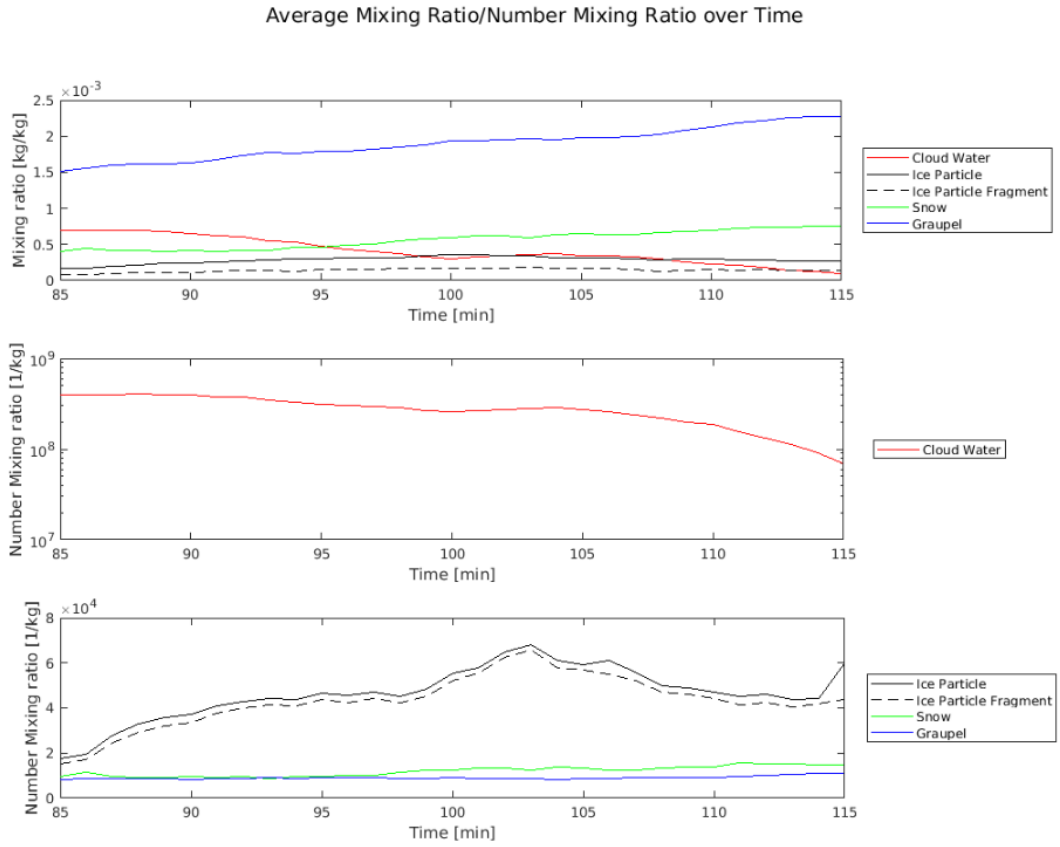

Fig. 15. *Conditionally averaged values from the mixed-phase region of the cloud (3 km to 9 km). The top picture shows the average mass concentration mixing ratio (kg/kg) over time for cloud water, ice particle, ice particle fragment, snow and graupel. The middle picture shows the average number concentration mixing ratio (1/kg) for cloud water. The bottom picture shows average number concentration mixing ratio (1/kg) over time for ice particles, ice particle fragments, snow and graupel.*

The evolution of the microphysical species in terms of mass concentration mixing ratio and number concentration mixing ratio averaged throughout the updraft (mixed-phase region) can be seen in Fig. 15. Cloud water shows a negative trend throughout the time-period which is consistent with what can be seen in the cartoon of snapshots. Ice particles and ice particle

fragments have a consistent mass concentration mixing ratio. Looking at the average number concentration mixing ratio for ice particles and ice particle fragments there is a positive trend from time-step 85 to almost 105 and then the number starts to decrease. Snows average mass concentration mixing ratio shows a positive trend while the number concentration mixing ratio is constant. Similar phenomena can be seen for graupel as with snow. As the mixing ratio of cloud droplets is decreasing and snow and graupel is increasing it is consistent with the ice-crystal process that ice particles, snow and graupel grows on behalf of cloud droplets.

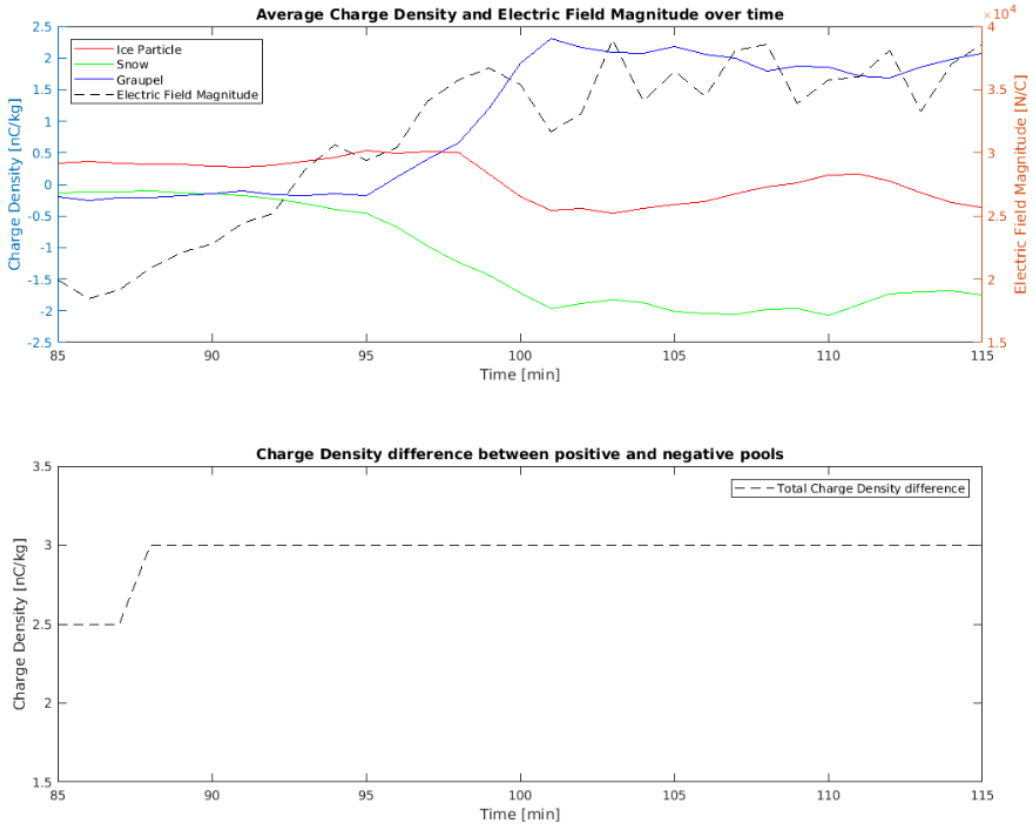

Fig. 16. *On the top picture the left y-axis is average charge density for ice particles, snow, graupel (nC/kg) over time. On the right y-axis the average magnitude of the electric field (N/C) over time. Bottom picture shows the difference in total charge density in terms of (nC/kg) between positively and negatively charged regions.*

The average charge density for ice particles, snow, graupel and average magnitude of the electric field are shown in the top plot in Fig. 16. The charge density difference was found to be stable and only change from 2.5 nC/kg to 3 nC/kg meanwhile the magnitude of the electric field is increasing steadily. The increase of the average magnitude of the electric field even though charge density difference remains stable can be explained by the fact that the region of the electric field is expanding.

From time-step 85 until 95 graupel and snow has a negative charge density while ice particles are positive. After time-step 95 graupel attains a positive charge density while snow is turning further negative. Ice particles turn negative just before time-step 100 and remain so until after 105, where they approach neutrally charged and then they turn negative again after 110. Snow and graupel remain negative and positive respectively after time-step 95. The electric field magnitude is steadily increasing just after time-step 85 until roughly time-step 100 which it starts to oscillate significantly. Comparing the average electric field magnitude to the snapshots of electric field seen in Fig. 8, 10, 12 and 14, even though the magnitude is higher in Fig. 8 and

10 the average is still higher in Fig. 12 and 14. The increase in magnitude of the electric field is consistent with the increase in charge density difference between positive and negative regions.

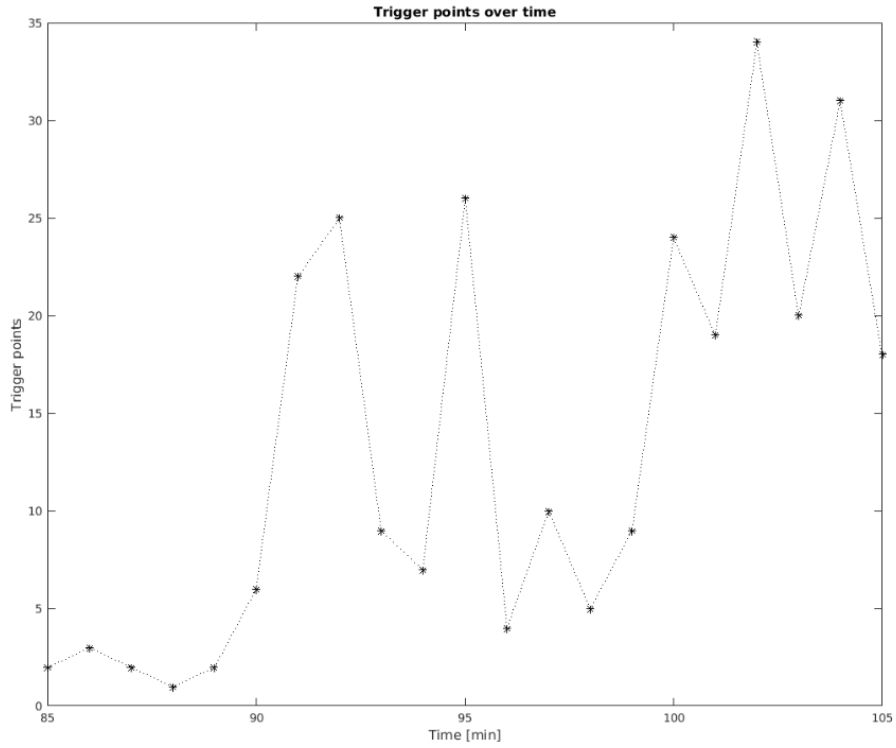

Fig. 17. *The x-axis shows time-steps in terms of minutes and the y-axis shows the amount of trigger points. The figure shows the amount of trigger points found within the convective updraft from time-step 85 (01:10 UTC) to 105 (01:30 UTC). The data is stored in such a way that all trigger points found between time-step 85 to 86 in intervals of 10 seconds is stored in time-step 85 and so on. Thus, the amount of lightning flashes shown in time-step 85 are all lightning flashes added from time-step 85:00, 85:10, 85:20, 85:30, 85:40, 85:50, 85:60. This applies to all other time-steps as well.*

The trigger points found within the convective cloud represents the location in the cloud where the trigger of the lightning flash occurred. As seen in Fig. 17. The lightning activity during the first five minutes are low compared to peak values found at time-step 95 (26 trigger points), 102 (34 trigger points) and 104 (31 trigger points). In a period of 20 minutes a total of 265 trigger points was recorded. The time between time-steps 90 to 95 and 100 to 105 can be considered high flash frequency compared to other time periods in this measurement. The amount of trigger points found throughout the period of 20 minutes gives a flash rate of 13.25 flashes per minutes. This is consistent with the flash rate of 10 flashes per minute Tessendorf (2007) found during a study on the entire storm system. This consistency validates that the electric properties of the AC-model are realistic.

Comparing charge densities, electric fields and charge density transferred to cloud in Fig. 10 and 12 it suggests that even though the peak value of electric field magnitude is weaker during time-step 105 compared to time-step 85 and 95 it was not followed by fewer flashes. However, comparing the average magnitude of the electric field (Fig. 16) to the amount of trigger points there seem to be a slight correlation with the increase average magnitude of the electric field the flash frequency seems to be higher. Hence, the amount of lightning flashes seems to be more dependent on average magnitude of the electric field than the peak value of the electric field.

5. Conclusion and outlook

In this project, the simulation of a thunderstorm cell was analysed both for microphysical and electrical quantities. The conclusions are as follows.

Ice particles, snow and graupel was found both positively and negatively charged for the first two time-steps, 85 and 95. At time-steps 105 and 115 ice particles and snow was found to be negatively charged while graupel positively charged. It was found that regions where graupel was charged positively/negatively, ice particles and snow were found to be negatively/positively charged. The charge acquired according to the model was compared with results found by Takahashi (1979). The charge found on graupel was consistent with what was found during Takahashi's (1979) experiment.

A correlation was found that the average magnitude of the electric field steadily increases when the difference in charge density between positively and negatively charged regions increase. This is expected as an increase in charge density difference would increase the electric potential which in turn increase the magnitude of the electric field. The increase of the average magnitude of the electric field was followed by an increase in amount of trigger points. Trigger points were found on altitudes of 6 km and 9 km on the downshear side of the updraft which were altitudes between differently charged regions. The amount of trigger points found during a 20-minute period was 265 giving a lightning flash rate of 13.25 per minute. The consistency between the trigger points found using the AC-model and the results by Tessendorf (2007) validates that the AC-model predictions of electrical properties are realistic.

As this analysis only covered one storm cell out of a multicellular storm future work that would be of interest would be to do the same analysis for the other storm cells to make comparisons and analyse differences of different cells within same storm system. It would also be interesting to look at which underlying properties results in intra-cloud, cloud-to-ground, and cloud-to-cloud lightning flash. As no atmospheric chemistry variables was considered neither for environment nor microspecies it would also be of interest to investigate properties that could follow from varying chemical contributions.

6. Bibliography

Ahren, C. D., and R. Henson, Meteorology Today An Introduction to Weather, Climate and the Environment, 11th edition, Ch. 5, 2015.

Holle, L. R., Annual rates of lightning fatalities by country, 20th International Lightning Detection Conference, 2008.

Holton, J., G. Hakim, An introduction to Dynamic Meteorology, 5th edition, Ch. 13, 2012.

Kitagawa, N., and M. Brook, A Comparison of Intracloud and Cloud-to-Ground Lightning Discharges, Journal of Geophysical Research, Vol. 65, 1189-1201, 1960.

Korolev, A. V., G. A. Isaac, S. G. Cober, J. W. Strapp, and J. Hallett, Microphysical characterization of mixed-phased clouds, Q. J. R. Meteorol. Soc., Vol. 129, 39-65, 2003.

Korolev, A. V., Limitations of the Wegener-Bergeron-Findeisen Mechanism in the Evolution of Mixed-Phase Clouds, J. Atmos. Sci., Vol 64, 3372-3375, 2007.

Lang, T. J., L. J. Miller, M. Weisman, S. A. Rutledge, L. J. Barker III, V. N. Bringi, V. Chandrasekar, A. Detwiler, N. Doesken, J. Helsdon, C. Knight, P. Krehbiel, W. A. Lyons, D. MacGorman, E. Rasmussen, W. Rison, D. Rust, and R. J. Thomas, The Severe Thunderstorm Electrification and Precipitation Study, Bull. Amer. Meteor. Soc., Vol. 85, 1107-1126, 2004.

Lin, Y., R. D. Farley, and H. D. Orville, Bulk Parameterization of the Snow Field in a Cloud Model, J. Climate Appl. Meteor., Vol. 22, 1065-1092, 1983.

Mossop, S. C. and Hallett, J., Ice Crystal Concentration in Cumulus Clouds: Influence of the Drop Spectrum, Journal of Science, Vol. 186, 632-634, 1974.

NLSI, National Lightning Safety Institute http://lightningsafety.com/nlsi_lls/nlsi_annual_usa_losses.htm Accessed: 2018-05-07

Phillips, V. T. J., P. J. DeMott, C. Andronache, K. A. Pratt, K. A. Prather, R. Subramanian, and C. Twohy, Improvements to an empirical parameterization of heterogeneous ice nucleation and its comparison with observations, J. Atmos. Sci., Vol. 70, 378-409, 2013.

Phillips, V. T. J., A. Khain, N. Benmoshe, and E. Ilotovitz, Theory of time-dependent freezing. Part I: Description of scheme for wet growth of hail. J. Atmos. Sci., Vol. 71, 4527-4557, 2014.

Phillips, V. T. J., M. Formenton, A. Bansemer, I. Kudzotsa, and B. Lienert, A scheme of sticking efficiency for collisions of snow and graupel with ice crystals: Theory and comparison with observations. J. Atmos. Sci., Vo.l 72, 4885-4902, 2015a.

Phillips, V. T. J., A. Khain, N. Benmoshe, E. Ilotovich, and A. Ryzhkov, Theory of time-dependent freezing and its application in a cloud model with spectral bin microphysics. II: Freezing raindrops and simulations. J. Atmos. Sci., Vol. 72, 262-286, 2015b.

Phillips, V. T. J., J. Yano, M. Formenton, E. Ilotoviz, V. Kanawade, I. Kudzotsa, J. Sun, A. Bansemer, A. G. Detwiler, A. Khain, and S. A. Tessendorf, Ice Multiplication by Breakup in Ice-Ice Collisions. Part II: Numerical Solutions, J. Atmos. Sci., Vol. 74, 2789-2811, 2017.

Pruppacher, H. R., Klett J. D., Microphysics of Clouds and Precipitation, Volume 18, 2nd edition, Ch. 18, 1997.

Reynolds, S. E., M. Brooks, and M. F. Gourley, Thunderstorm Charge Separation, Journal of Meteorology, Vol 14, 426-436, 1957.

Rogers, R. R., Yau, M. K., A Short Course in Cloud Physics, 3rd edition, 1989.

Stull, R. B., Meteorology for Scientists and Engineers, 2nd edition, Ch. 15, 2000.

Tessendorf, S. A., S. A. Rutledge, and K. C. Wiens, Radar and Lightning Observations of Normal and Inverted Polarity Multicellular Storms from STEPS, Monthly Weather Review, Vol 135, 3682-3706, 2007.

UCAR, University Corporation for Atmospheric Research
www.unidata.ucar.edu/software/netcdf/

Young, H. D., R. A. Freedman, and A. L. Ford, University Physics With Modern Physics, 13th edition, Ch. 21, 2011.

Appendix A – Definitions and technical description of meteorological terms

Cloud water

Droplet of water with a size range between $(10 - 100\mu m)$.

Cold-based cloud

The base of a cloud has a temperature of 0℃ or lower.

Cold-rain process

Precipitation is formed only by the ice-crystal process.

Cumuliform cloud

Cloud with vertical development and updraft speed higher than $1\ m/s$.

Downdraft

Downward going wind.

Graupel

Ice formation which has grown due to accretion of supercooled droplets.

Ice crystal process

Diffusional growth of ice crystals due to supersaturation relative to water vapour.

Ice particle/Ice crystal

Frozen cloud droplet. Also referred to as ice crystal and cloud ice.

Ice particle/Ice crystal fragment

Fragment from ice particles due to shattering from collision.

Lightning leader

A channel propagating through the air composed of ions,

Microphysical specie

A collection word for different phases, shapes and size of water that can be found within a cloud.

Mixed-phased region

Region in a cloud between $0℃$ and $-36℃$ where all microphysical species can exist.

Mass mixing ration

The mass of one component relative to other components found in specified region.

Number mixing ratio

The number of components that can be found in a specified region.

Snow

Aggregate of ice particles.

Stratiform cloud

Clouds with a horizontal development. Updraft speeds does not exceed $1\ m/s$.

Supercooled droplet

A cloud droplet in liquid phase that has a temperature below $0℃$.

Trigger point

Point in space that triggers a lightning flash.

Updraft

Upward going wind.

Warm-based cloud

The base of a cloud has a temperature of $0℃$ or higher.

Appendix B – Preview of scripts and programs

Shell script

```
#!/bin/sh
# Template to create NetCDF file for a variable:
# ncrcat -O -v <Variable_name> Time,1,10000 <NetCDF_Data> ./<Output_file>

set echo
# Vertical velocity
ncrcat -O -v W -d Time,1,10000 wrfout_d01_2000-06-19_23:45:00
./wrfout_d01_2000-06-19_23:45:00_W.nc
# Charge density to cloud
ncrcat -O -v CHARGEDENS2CLD -d Time,1,10000 wrfout_d01_2000-06-19_23:45:00
./wrfout_d01_2000-06-19_23:45:00_CHARGEDENS2CLD.nc
# Temperature
ncrcat -O -v TEMP -d Time,1,10000 wrfout_d01_2000-06-19_23:45:00
./wrfout_d01_2000-06-19_23:45:00_TEMP.nc
```

Fortran90 program

```
program hist
        use netcdf
        implicit none
        !-----DECLARATION OF VARIABLES----------------------------
        integer :: i,j, t, lifetime,   ist, bt, ew, ns
        integer :: k, is
        parameter ( ist=126, bt = 40, ew=80, ns=80)
        real, allocatable :: QCLOUD(:,:,:,:)
        !-------------------------------------------------------
        allocate (QCLOUD(ew,ns,bt,ist))
    call read_wrf4d_output('QCLOUD', 6 , QCLOUD)
  !-----CREATES FILE FROM DATA-----------------------------
    open(1,file='QCLOUD_SN56_T120',form="formatted",
access="sequential",status="unknown")
        j = 57
        is = 121
        do i=1,ew
                do k=1,bt
                        write(1,*) QCLOUD(i,j,k,is), i, k
                enddo
        enddo
        close(1)
  !-------------------------------------------------------
    stop
        CONTAINS
        SUBROUTINE read_wrf4d_output(var, nvar, WRFVAR)
                integer, intent(in) ::  nvar
                character (len=nvar), intent(in) :: var
                real , Dimension(ew,ns,bt,ist), intent(out):: WRFVAR
                integer :: wrf_ncid, wrf_varid
```

```
                character  (len = *), parameter :: &
                        wrfout_file="wrfout_d01_2000-06-19_23:45:00"
                print*, wrfout_file//'_'//var//'.nc'
! Open the file. NF90_NOWRITE tells netCDF we want read-only access to
! the file.
call check( nf90_open(wrfout_file//'_'//var//'.nc', NF90_NOWRITE, wrf_ncid) )
                print*, var
                ! Get the varid of the data variable, based on its name.
                call check( nf90_inq_varid(wrf_ncid, var, wrf_varid) )
                ! Read the data.
                print*, "reading::", var
                call check( nf90_get_var(wrf_ncid, wrf_varid, WRFVAR) )

end subroutine read_wrf4d_output
subroutine check(status)
                integer, intent ( in) :: status
                if(status /= nf90_noerr) then
                        print *, trim(nf90_strerror(status))
                        stop "Stopped"
                end if
end subroutine check

end
```

MATLAB script

```
clear all
clc

% CLOUD WATER mixing ratio vertical slice
QCLOUD = load('QCLOUD_SN56_T85');

k = 1
for i=1:80
   for j=1:40
      z1_km(j) = j/2 + 0.65
      x1_km(i) = i
      QCLOUD_v(j,i) = QCLOUD(k,1);
      if(i ~= QCLOUD(k,2))
         exit
      end
      if(j ~= QCLOUD(k,3))
         exit
      end
      k = k + 1;
   end
end

figure
subplot(3,2,1)
isolevels = linspace(0,0.005,20)
[c,h] = contourf(x1_km, z1_km, QCLOUD_v, isolevels, 'edgecolor','none');
clabel(c, h, 'FontSize', 15, 'Rotation', 0);
h = colorbar; set(h, 'fontsize', 14);
caxis([0 0.005])
title('Cloud water mixing ratio [kg/kg]', 'FontSize', 20)
```

```
xlabel('x (km)', 'FontSize', 20)
ylabel('z (km)', 'FontSize', 20)
axis([30 70 1.3 15]);
hold on

% Vertical velocity vertical slice
W = load('W_SN56_T85');

k = 1
for i=1:80
   for j=1:41
      z6_km(j) = j/2 + 0.65
      x6_km(i) = i
      W6_v(j,i) = W(k,1);
      if(i ~= W(k,2))
         exit
      end
      if(j ~= W(k,3))
         exit
      end
      k = k + 1;
   end
end

isolevels2 = linspace(-9,19,15)
[c,h] = contour(x6_km, z6_km, W6_v, isolevels2, 'k-');
clabel(c, h, 'FontSize', 15, 'Rotation', 0);
%h = colorbar; set(h, 'fontsize', 14);
%caxis([-10 20])
title('Cloud Water Mixing Ratio [kg/kg] and Vertical Velocity [m/s]', 'FontSize', 15)
legend('Cloud Water Mixing Ratio','Vertical Velocity')
xlabel('x (km)', 'FontSize', 20)
```

```
ylabel('MSL (km)', 'FontSize', 20)
axis([30 70 1.3 15]);
hold off
```